E-ISSN 2586-9027
Homepage : https://tci-thaijo.org/index.php/SciTechAsia Science & Technology Asia
Vol.30 No.3 July - September 2025 Page: [13-20]
Original research article

Catalytic System Improvement Through Computational Approaches

Phanchita Wuttikorn, Pinapa Suttiphong,
Surachet Thongboon, Kulpavee Jitapunkul*

Department of Chemical Engineering, Faculty of Engineering, Kasetsart University, Bangkok 10900, Thailand

Received 30 May 2025; Received in revised form 13 July 2025
Accepted 29 July 2025; Available online 30 September 2025

ABSTRACT

This research aims to develop a predictive model for hydrogen production using a titanium dioxide-based (TiO_2) photocatalyst through an artificial neural network (ANN). The primary objective is to enhance photocatalyst design for efficient hydrogen production, supporting the transition from fossil fuels to clean hydrogen energy while reducing carbon dioxide emissions. The project consists of two parts: machine learning and experimental studies, with a primary focus on the first. In Part 1, machine learning is used to build a predictive model for hydrogen production, utilizing TiO_2-based photocatalysts. Pearson correlation is applied to select direct and indirect parameters that significantly impact hydrogen production. Data normalization is performed to minimize variations, and the dataset (122 direct parameter samples and 169 indirect parameter samples) is split by using k-fold cross validation and after that into training (80%), testing (10%), and validation (10%) sets before model training begins. The accuracy of the model is evaluated using R-squared and Root Mean Square Error (RMSE). Part 2 involves experimental work focusing on methane-to-ethane conversion using the same TiO_2-based photocatalyst. The study compares different silver concentrations to determine the most efficient composition for ethane production. While both parts are crucial, the primary emphasis remains on hydrogen production and predictive modeling, as machine learning plays a key role in optimizing photocatalyst design and improving hydrogen yield predictions.

Keywords: Artificial Neuron Network (ANN); Direct Parameters; Hydrogen Production; Indirect Parameters; Methane Conversion; Pearson's Correlation; Photo-deposition; TiO_2-base Photocatalyst; Titanium Dioxide

***Corresponding author:** fengkvj@ku.ac.th **doi:** 10.14456/scitechasia.2025.42

1. Introduction

Hydrogen is a clean, renewable fuel with high energy potential, making it a promising alternative to fossil fuels. It is widely used in transportation, aerospace, oil refining, fertilizer production, and chemical manufacturing [1, 2]. With no greenhouse gas emissions and a high energy yield per unit mass, hydrogen offers a sustainable solution for addressing climate change and reducing fossil fuel dependency [1].

However, hydrogen production often involves reactions with high activation energy or slow kinetics, requiring effective catalysts. Titanium dioxide (TiO_2) is a commonly used photocatalyst due to its chemical stability, low reactivity, environmental safety, and affordability [3, 4]. Its broad light absorption and long lifespan further supports its application in photocatalysis [5].

To enhance TiO_2 performance, metal doping particularly with platinum (Pt) is employed. Pt-doped TiO_2 improves charge separation, expands light absorption, and increases surface area and active sites, boosting photocatalytic efficiency [6]. Given the abundance of experimental data, Pt-doped TiO_2 is also suitable for predictive modeling using Machine Learning (ML) [7, 8].

Artificial Neural Networks (ANN) offer an efficient approach to model hydrogen production, reducing the need for extensive experimentation and minimizing time, cost, and human error [7, 9].

In addition to water splitting, hydrogen is also produced as a by-product during the conversion of methane to ethane. Ethane is a key feedstock in the production of ethylene, widely used in plastics and chemicals [10, 11]. TiO_2-based photocatalysis provides a sustainable and energy-efficient method for methane conversion, offering both environmental benefits and valuable chemical outputs [12].

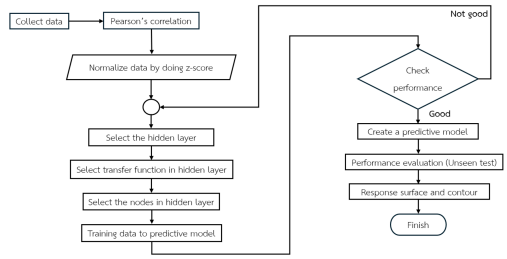

Fig. 1. Flowchart for machine learning.

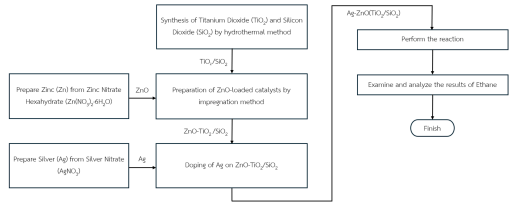

Fig. 2. Flowchart for the experiment.

2. Materials and Methods

2.1 Machine learning

Start with data collection and Pearson's correlation analysis to identify significant variables, followed by z-score normalization. An Artificial Neural Network (ANN) is then configured by selecting hidden layers, activation functions, and the number of nodes. The model is trained and its performance evaluated; if unsatisfactory, the configuration is adjusted and retrained. Once optimized, the model is validated using unseen data and used to generate response surface and contour plots to visualize the effects of input variables on the output [8].

2.2 Experiment

Titanium dioxide (TiO_2) and silicon dioxide (SiO_2) were synthesized via the hydrothermal method from Tetrabutyl titanate (TBT) and Tetraethyl orthosilicate (TEOS), respectively. Zinc oxide (ZnO) was subse-

Table 1. Differences in Procedures of Batch 1 and Batch 2.

Steps	Batch 1	Batch 2
Addition of TBT	Added all at once	Added drop by drop
Dope Ag	Directly dope into ZnO-(TiO_2/SiO_2)	Use the photo-deposition method before doping it into ZnO-(TiO_2/SiO_2)

quently loaded onto the catalyst using the impregnation method, followed by silver (Ag) doping. The catalyst was then employed in the ethane conversion reaction, with experiments conducted in two batches as described in Table 1 [13, 14].

3. Results and Discussion

3.1 Machine learning

3.1.1 Parameter selection

We used Pearson's correlation for feature selection to identify parameters that influence hydrogen production. This method can elucidate both direct and indirect relationships between input parameters and hydrogen production. In a direct relationship, the correlation coefficient (r) indicates how a specific input parameter directly influences the amount of hydrogen produced. Conversely, an indirect relationship reveals how input parameters affect each other first, and subsequently, how these interdependencies impact hydrogen production. This comprehensive analysis involves generating a Pearson correlation matrix, which displays the correlation coefficients for every pair of variables in the dataset. Understanding these direct and indirect influences is crucial for feature selection, allowing us to identify the most significant input parameters for developing robust predictive models of hydrogen production [15].

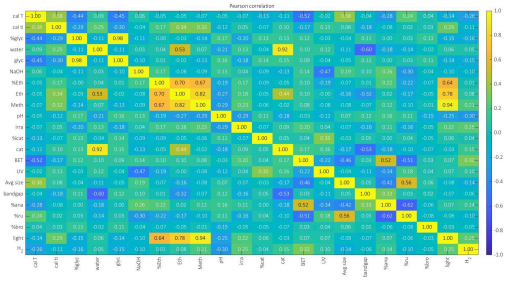

Fig. 3. Pearson's correlation matrix.

To identify direct input parameters affecting hydrogen production, selection criteria were set: a positive correlation ≥ 0.20 or a negative correlation ≤ -0.20. Based on this, six parameters were selected: calcination temperature, methanol amount, pH, irradiation time, BET surface area, and light power. Among these, calcination temperature and pH met the negative correlation criterion. The selected parameters are categorized into two groups: (1) Catalyst preparation: calcination temperature, pH, and BET surface area; and (2) Catalytic reaction: methanol amount, irradiation time, and light power. Indirect parameters were then identified based on a strong correlation (≥ 0.5 or ≤ -0.5) with the selected direct parameters. While these have limited direct influence on hydrogen production, they significantly affect the direct parameters. After that combined, the direct and indirect parameters are grouped into two categories: (1) Catalyst preparation: calcination temperature, pH, water, bandgap, average particle size, BET surface area, %anatase, and %rutile; and (2) Catalytic reaction: methanol, ethanol, irradiation time, catalyst loading, and light power. From Fig. 3, we can see an indirect relationship: methanol significantly impacts light power, which in turn affects hydrogen production, though to a lesser extent.

```
Data for ANN and data left for final testing are divided
Selected models have been saved!
Predictions using selected models have been saved!
Unseen Test R2: 0.50637
Unseen Test RMSE: 0.38556
selected network Train R2: 0.78698
selected network Train RMSE: 0.48371
selected network Test R2: 0.5193
selected network Test RMSE: 0.7324
Plotting complete.
```

Fig. 4. R^2 and RMSE of average models and unseen test.

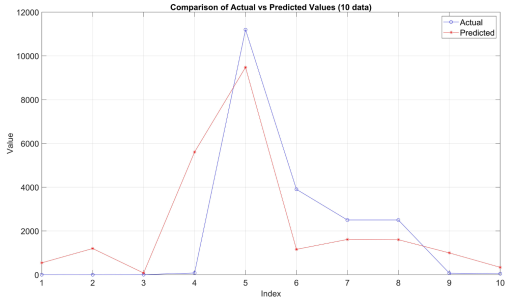

Fig. 5. Comparison between actual and predict H_2.

3.1.2 Create a predictive model and predict unseen test

The data used was normalized before undergoing the training process [16]. The model was developed using a single hidden layer with 60 nodes and trained on 122 data samples using the Bayesian regularization backpropagation algorithm (trainbr). The hyperbolic tangent sigmoid (tansig) function was applied as the transfer function. A 3-fold cross-validation approach was used, with the dataset split into 80% for training, 10% for validation, and 10% for testing. Subsequently, models from fold 1 and fold 2 with $R^2 > 0.46$, and from fold 3 with $R^2 > 0.65$, were selected and averaged to create a predictive model with high generalization capability [9, 17].

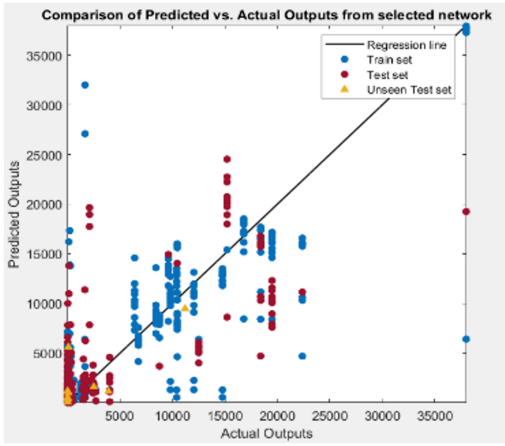

Fig. 6. Regression plot for hydrogen yield prediction.

It can be observed that the predicted hydrogen values follow the same trend as the actual values. However, the differences in their magnitudes result in a relatively low R^2 value.

This scatter plot compares predicted and actual hydrogen outputs from a trained neural network. The black diagonal indicates perfect predictions, with blue dots for training data, red for the test set, and yellow triangles for unseen data. While predictions generally follow the actual trend, deviations from the diagonal reveal limited accuracy. These discrepancies result in a relatively low R^2 value, indicating the model captures overall patterns but lacks precision, underscoring the need for improved generalization and accuracy.

The poor results might stem from an unsuitable model choice, likely because of limited data. You could try switching from Neural Networks to Random Forest (RF), Support Vector Machine (SVM), or other alternatives.

3.1.3 Response surface and contour plot

1. Catalyst preparation

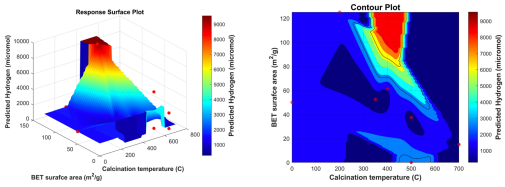

Fig. 7. Calcination temperature and BET surface area.

The optimal range was found to be 350–450 °C for calcination temperature and 90-120 m^2/g for BET surface area.

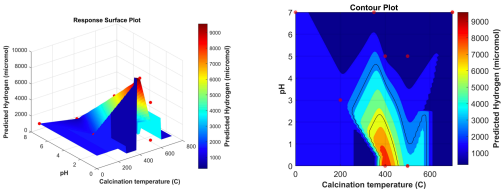

Fig. 8. Calcination temperature and pH.

The optimal range was found to be 380–420 °C for calcination temperature and 0-1 for pH.

2. Catalytic reaction

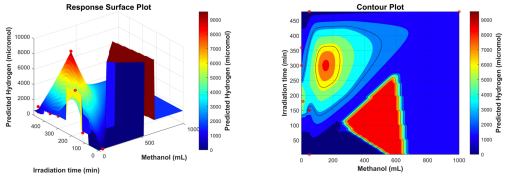

Fig. 9. Methanol and irradiation time.

The optimal range was found to be 270–330 mins for irradiation time and 150-180 mL for methanol.

3. Between Catalyst preparation and Catalytic reaction relationships

The optimal range was found to be 380–420 °C for calcination temperature and 120-180 mL for methanol.

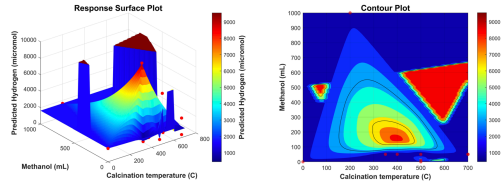

Fig. 10. Calcination temperature and methanol.

Table 2. Added TBT (Tetrabutyl Titanate) all at once and directly doped it into ZnO-(TiO_2/SiO_2) in Batch 1.

Ratios		% Ag	Cat (g)	t (h)	C_2H_6 (μmol/g·h)	%CH_4 conversion ($\times10^{-4}$)
TiO_2	SiO_2					
1	1	0.5	0.10	3	0.00	0.00
1	2				7.50	3.27
1	3				10.28	4.48
1	5				25.82	11.25
1	10				0.93	0.40
1	5	0.5	0.10	1	21.44	3.11
				2	27.82	8.08
				3	23.14	10.08
1	5	0.25	0.20	1	10.39	3.01
				2	6.70	3.89
				3	7.58	6.61

Note: t = Time of result collection (h), cat = Catalyst loading (g).

3.2 Experiment

From Table 2, the data can be analyzed into three cases.

In Case 1, varying TiO_2/SiO_2 ratios with fixed 0.50% Ag, 0.1 g catalyst, and 3-hour reaction time yielded a maximum ethane production of 27.8224 $\mu mol \cdot g^{-1} \cdot h^{-1}$ and a methane conversion rate of 11.25×10^{-4}%. In Case 2, with a fixed TiO_2:SiO_2 ratio of 1:5, 0.50% Ag, and 0.1 g catalyst, varying the reaction time showed the highest ethane yield at 2 hours 27.8224 $\mu mol \cdot g^{-1} \cdot h^{-1}$ and a conversion rate of 8.08×10^{-4} %. In Case 3, under the same TiO_2:SiO_2 ratio but with 0.25% Ag and 0.2 g catalyst, the peak ethane yield was $10.3905 \mu mol \cdot g^{-1} \cdot h^{-1}$ at 1 hour, with a conversion rate of 3.01×10^{-4} %. It can be observed that at a TiO_2:SiO_2 ratio of 1:5, the %methane conversion increases with time,

Table 3. Added TBT (Tetrabutyl Titanate) drop by drop. Use the photo-deposition method before doping into ZnO-(TiO_2/SiO_2) in Batch 2 [18, 19].

Ratios		% Ag	Cat (g)	t (h)	C_2H_6 (μmol/g·h)	%CH_4 conversion ($\times10^{-4}$)
TiO_2	SiO_2					
1	3	1	0.10	1	12.71	1.85
					6.70	1.95
					5.30	2.31
1	5	1	0.10		28.57	4.15
					13.90	4.04
				3	7.30	3.18
1	1	0.5	0.10	3	23.30	10.15
1	2			3	9.64	4.20
1	3			3	22.89	9.97
				3	15.64	6.82
				3	7.58	6.61

Note: t = Time of result collection (h), cat = Catalyst loading (g).

as methane is consumed in the reaction to convert it into ethane. However, once the equilibrium point is reached (at a TiO_2:SiO_2 ratio of 1:10), very little methane is required for conversion to ethane.

From Table 3, the data can be analyzed into three cases.

In Case 1, with a fixed TiO_2:SiO_2 ratio of 1:3, 1% Ag, and 0.1 g catalyst, varying the reaction time showed the highest ethane yield at 1 hour 12.7166 μmol·g^{-1}·h^{-1} with a methane conversion rate of 1.85×10^{-4} %. In Case 2, under the same conditions but with a 1:5 TiO_2:SiO_2 ratio, the highest ethane yield was 28.5722 μmol·g^{-1}·h^{-1} at 1 hour, with a conversion rate of 4.15×10^{-4} %. In Case 3, varying TiO_2:SiO_2 ratios with 0.50% Ag, 0.1 g catalyst, and 3-hour reaction time, the peak ethane yield was 27.8224 μmol·g^{-1}·h^{-1} and the conversion rate was 11.25×10^{-4} %. It can be observed that for the TiO_2:SiO_2 ratio of 1:5, with 1% Ag and a catalyst loading of 0.10 g, the %methane conversion decreases as time increases. The most probable reason for this is catalyst deactivation, such as coking or sintering, which rapidly reduces the catalyst's efficiency over time, thereby diminishing its ability to convert methane after the 1-hour mark.

4. Conclusion

4.1 Machine learning

A hydrogen production prediction model was developed using six input parameters including calcination temperature, methanol (mL), pH, irradiation time, BET surface area, and light power and one output (hydrogen). The model featured a single hidden layer with 60 nodes, Bayesian regularization training, and a tangent sigmoid transfer function. Given the small dataset, 3-fold cross-validation was applied. On unseen test data, the model achieved improved accuracy with an R^2 of 0.51 and RMSE of 0.39. Response Surface and Contour Plots identified optimal input ranges, aligning with theory in most cases. However, some discrepancies emerged: the model predicted an optimal pH of 0–1, below the theoretical 3–5 range, and no clear optimum for methanol or light power. A similar method was applied to indirect parameters, but due to consistently low R^2 values, only selected plots were included.

To effectively apply machine learning in this study, the dataset should first be classified to account for the diverse range of metal doping types. Increasing the volume of data is essential to enhance the performance and reliability of the Artificial Neural Network (ANN). Additionally, the data should be validated against theoretical expectations to ensure consistency and scientific accuracy. Finally, selecting an appropriate machine learning model tailored to the dataset characteristics is crucial for generating meaningful and predictive results.

4.2 Experiment

This study synthesized and evaluated TiO_2-based photocatalysts for methane-to-ethane conversion using Ag–ZnO-(TiO_2/SiO_2) composites across two experimental batches. In Batch 1, TBT (Tetrabutyl Titanate) was added all at once and directly doped into ZnO–(TiO_2/SiO_2), while in Batch 2, TBT was added dropwise via photo-deposition prior to doping. Both batches varied TiO_2/SiO_2 ratios, reaction times, catalyst loadings, and Ag percentages to identify optimal conditions. Overall, Batch 2 showed higher ethane yields, except in Batch 1 at a TiO_2:SiO_2 ratio of 1:5, which produced 25.8260 μmol·g^{-1}·h^{-1} ethane and a methane conversion rate of 11.25 $\times10^{-4}$%. The highest ethane yield in Batch 1 (27.8224 μmol·g^{-1}·h^{-1}) occurred at the same ratio, with 0.5% Ag, 0.1 g catalyst, and 2 hours of reaction. However, the overall highest yield was in Batch 2 under the same TiO_2:SiO_2 ratio, with 1% Ag, 0.1 g catalyst, and 1-hour reaction time, yielding 28.5722 μmol·g^{-1}·h^{-1} and a conversion rate of 4.15 $\times10^{-4}$%. These results suggest that photo-deposition with controlled TBT addition significantly improves catalyst performance.

Extending the duration of the experiments allows for a more comprehensive evaluation of catalyst performance across varying conditions. Experimental parameters identified in the machine learning analysis should be systematically varied to assess their influence on outcomes. Furthermore, machine learning techniques can be applied to the experimental results to identify key factors driving ethane production and methane conversion, ultimately guiding optimization of the catalytic process.

Acknowledgements

We would like to express our gratitude to the Faculty of Engineering, Department of Chemical Engineering, Kasetsart University, for providing financial support, research facilities, and equipment used in this study. In addition, this research was also financially supported by Fundamental Fund under the Kasetsart University Research and Development Institute (KURDI) (Grant No. FF(KU)51.67). Thus, we would like to express our sincere gratitude to the Kasetsart University Research and Development Institute.

References

[1] Ali I, Imanova GT, Mbianda XY, Alharbi OML. Role of the radiations in water splitting for hydrogen generation. Sustain Energy Technol Assess 2022; 51:101926.

[2] Rafique M, Hajra S, Irshad M, Usman M, Imran M, Assiri MA, Ashraf WM. Hydrogen production using TiO_2-based photocatalysts: a comprehensive review. ACS Omega 2023; 8:25640-8.

[3] Gahlot S, Dappozze F, Mishra S, Guillard C. High surface area g-C_3N_4 and g-C_3N_4-TiO_2 photocatalytic activity under UV and visible light. J Environ Chem Eng 2021; 9:105587.

[4] Hoffmann MR, Martin ST, Choi W, Bahnemann DW. Environmental applications of semiconductor photocatalysis. Chem Rev 1995; 95:69-96.

[5] Fujishima A, Honda K. Electrochemical photolysis of water at a semiconductor electrode. Nature 1972; 238:37-8.

[6] Jovic V, Al-Azri ZHN, Chen W-T, Sun-Waterhouse D, Idriss H, Waterhouse GIN. Photocatalytic H□ production from ethanol–water mixtures over Pt/TiO_2 and Au/TiO_2 photocatalysts: a comparative study. Top Catal 2013; 56:1139-51.

[7] AWS. What is the neural network? [Internet]. [cited 2025 May 27]. Available from: https://aws.amazon.com/th/what-is/neural-network/

[8] Wilson S. Artificial intelligent insights. Machine learning. [Internet]. [cited 2025 May 27]. Available from: https://ai2people.com/machine-learning

[9] Mohruni AS. Algorithm. [cited 2025 May 27]. Available from: https://repository.unsri.ac.id/97951/1/Ithenticate_Levenberg_Marquardt__Bayesian_regularization__and_.pdf

[10] Sciencedirect. Ethane. [cited 2025 May 27]. Available from: https://www.sciencedirect.com/topics/earth-and-planetary-sciences/ethane

[11] Springer Nature. Methane. [cited 2025 May 27]. Available from: https://link.springer.com/article/10.1007/-BF02208779

[12] Bo C, Liu J, Zhang Y, Chang H, Zhang X, Liu X, Chen C, Piao L. Effective photocatalytic methane oxidation over the TiO_2/methanotrophs system. Nano Today 2023; 52:101938.

[13] Bloch E, Phan T, Bertin D, Llewellyn P, Hornebecq V. Direct synthesis of mesoporous silica presenting large and tunable pores using BAB triblock copolymers. Microporous Mesoporous Mater 2008; 112:612-20.

[14] Dubey RS, Rajesh YBRD, More MA. Synthesis and characterization of SiO_2 nanoparticles via sol-gel method for industrial applications. Mater Today Proc 2015; 2:3575-9.

[15] Hayes, A. F. Introduction to Mediation, Moderation, and Conditional Process Analysis: A Regression-Based Approach (2nd ed.). The Guilford Press. [cited 2025 July 11]. Available from: https://www.scirp.org/reference/referencespapers?referenceid=3016713

[16] Statology. Z-Score Normalization Explained. [cited 2025 July 12]. Available from: https://www.statology.org/z-score-normalization/

[17] Reference to an electronic data source: Antoniadis P. Tangent sigmoid. [cited 2025 May 27]. Available from: https://www.baeldung.com/cs/sigmoid-vs-tanh-functions

[18] Abbad S, Guergouri K, Gazaout S, Djebabra S, Zertal A, Barille R, Zaabat M. Effect of silver doping on the photocatalytic activity of TiO_2 nanopowders synthesized by the sol-gel route. J Environ Chem Eng 2020; 8:103718.

[19] Ortega-Granados JA, Thangarasu P. Photo-deposition of Ag/AuNPs on TiO_2 accelerating the oxidation of tetracycline under visible light. Mater Lett 2022; 321:132455.